Articles

Unusual C−H Allylic Activation in the {Pt^{II}(cod)} Fragment Bonded to a {$Pt_2(\mu\text{-}S)_2$} Core

Rubén Mas-Ballesté,[†] Paul A. Champkin,[‡] William Clegg,[‡] Pilar González-Duarte,*[,†] Agustí Lledós,*[,†] and Gregori Ujaque[†]

Departament de Química, Universitat Autònoma de Barcelona, E-08193 Bellaterra, Barcelona, Spain, and School of Natural Sciences (Chemistry), University of Newcastle, Newcastle upon Tyne NE1 7RU, U.K.

Received November 21, 2003

Complexes [{$Pt_2(\mu_3\text{-}S)_2$(dppp)$_2$}Pt(cod)]Cl_2 (**1**) and [{$Pt_2(\mu_3\text{-}S)_2$(cod)$_2$}Pt(dppp)]Cl_2 (**3**), where dppp = 1,3-bis(diphenylphosphino)propane and cod = 1,5-cyclooctadiene, have been synthesized by reacting [$Pt_2(\mu\text{-}S)_2$(dppp)$_2$] and [$PtCl_2$(cod)] (1:1), and [$Pt(SH)_2$(dppp)] and [$PtCl_2$-(cod)] (1:2), respectively. Complex **1** has not allowed substitution of cod by the chelating dppp ligand. Remarkably, the reaction of **1** with methoxide anion yields [{$Pt_2(\mu_3\text{-}S)_2$(dppp)$_2$}-Pt(C_8H_{11})]Cl (**2**), which entails deprotonation of cod instead of the nucleophilic attack of CH_3O^- on the olefinic bond. In addition, replacement of the deprotonated cod ligand in **2** by dppp has not been achieved. A combination of experimental data and DFT calculations in **2** is consistent with the binding of $C_8H_{11}^-$ to platinum(II) by means of one η^2-alkene and one η^1-allyl bond. The structures of **1** and **2** have been confirmed by single-crystal X-ray diffraction. Analogous to **1**, the reaction of **3** with sodium methoxide causes the subsequent deprotonation of the two cod ligands, yielding [{$Pt_2(\mu_3\text{-}S)_2$(cod)(C_8H_{11})}Pt(dppp)]Cl (**4**) and [{$Pt_2(\mu_3\text{-}S)_2$(C_8H_{11})$_2$}Pt(dppp)] (**5**). In contrast to **1**, replacement of cod by dppp in **3** and **4** leads to **1** and **2**, respectively. Also, the substitution of one $C_8H_{11}^-$ ligand by dppp in **5** leads to **2**. On the basis of DFT calculations, with inclusion of solvent effects, the factors governing the chemical behavior of the {Pt(cod)}$^{2+}$ fragment bonded to a [$Pt_2(\mu\text{-}S)_2L_4$] (L_2 = dppp, cod, or $C_8H_{11}^-$) metalloligand are discussed.

Introduction

Activation of the C−H bond in olefins bound to metal centers is relevant in organometallic chemistry because of its significance in many catalytic processes.[1] Frequently, this activation is achieved by reacting the metal-olefin complex with a base. However, this reaction may cause not only deprotonation of the olefin but, alternatively, the nucleophilic attack of the base to the double bond.[2] Both reactions are depicted in Scheme 1 for a {Pt(η^2-propene)} fragment, where for the deprotonation reaction only the more usual C−H allylic activation has been taken into account. While the nucleophilic attack at olefinic bonds coordinated to palladium(II) and platinum(II) has been well studied, unlike palladium, examples of base-promoted olefin deprotonation reactions in neutral platinum-olefin complexes are very scarce.[3] In addition, the study of the reactivity of cationic platinum-olefin complexes, which show an enhanced electrophilicity at the olefinic moiety,[4,3] has often been hampered by the lability of the unsaturated ligand in these complexes.[5] With respect to the {M^{II}(cod)} fragment in palladium or platinum complexes, the reaction with a wide range of bases has led in most cases to the nucleophilic attack of these species to the olefinic bonds,[6] base-promoted deprotonation being observed only if the attacking species is a tertiary amine.[7]

In the quest to explore the remarkable chemistry of the {$Pt_2(\mu\text{-}S)_2$} core, its influence on the reactivity of a {Pt^{II}(cod)} fragment attracted our interest. The striking

* Corresponding authors.
[†] Universitat Autònoma de Barcelona.
[‡] University of Newcastle.

(1) Crabtree, R. H. *The Organometallic Chemistry of the Transition Metals*; John Wiley and Sons: New York, 2001.
(2) (a) Hahn, C.; Morvillo, P.; Herdtweck, E.; Vitagliano, A. *Organometallics* **2002**, *21*, 1807. (b) Vicente, J.; Chicote, M.-T.; MacBeath, C.; Fernández-Baeza, J.; Bautista, D. *Organometallics* **1999**, *18*, 2677. (c) Hamed, O.; Henry, P. M. *Organometallics* **1997**, *16*, 4903.
(3) Bandoli, G.; Dolmella, A.; Fanizzi, F. P.; Di Masi, N. G.; Maresca, L.; Natile, G. *Organometallics* **2002**, *21*, 4595.
(4) Bandoli, G.; Dolmella, A.; Di Masi, N. G.; Fanizzi, F. P.; Maresca, L.; Natile, G. *Organometallics* **2001**, *20*, 805.
(5) (a) Albietz, P. J.; Yang, K.; Lachicotte, R. J.; Eisenberg, R. *Organometallics* **2000**, *19*, 3543. (b) Fusto, M.; Giordano, F.; Orabona, I.; Ruffo, F.; Panunzi, A. *Organometallics* **1997**, *16*, 5981.
(6) (a) Macchioni, A.; Bellachioma, G.; Cardaci, G.; Travaglia, M.; Zuccacia, C.; Milani, B.; Corso, G.; Zangrado, E.; Mestroni, G.; Carfagna, C.; Formica, M. *Organometallics* **1999**, *18*, 2677. (b) Hoel, G. R.; Stockland, R. A.; Anderson, G. K.; Ladipo, F. T.; Braddock-Wilking, J.; Rath, N. P.; Mareque-Rivas, J. C. *Organometallics* **1998**, *17*, 1155.
(7) (a) Peters, J. C.; Harkins, S. B.; Brown, S. D.; Day, M. W. *Inorg. Chem.* **2001**, *40*, 5083. (b) Dahan, F.; Agami, C.; Levisalles, J.; Rose-Munch, F. *Chem. Commun.* **1974**, 505.

10.1021/om034312x CCC: $27.50
Publication on Web 04/17/2004

Scheme 1

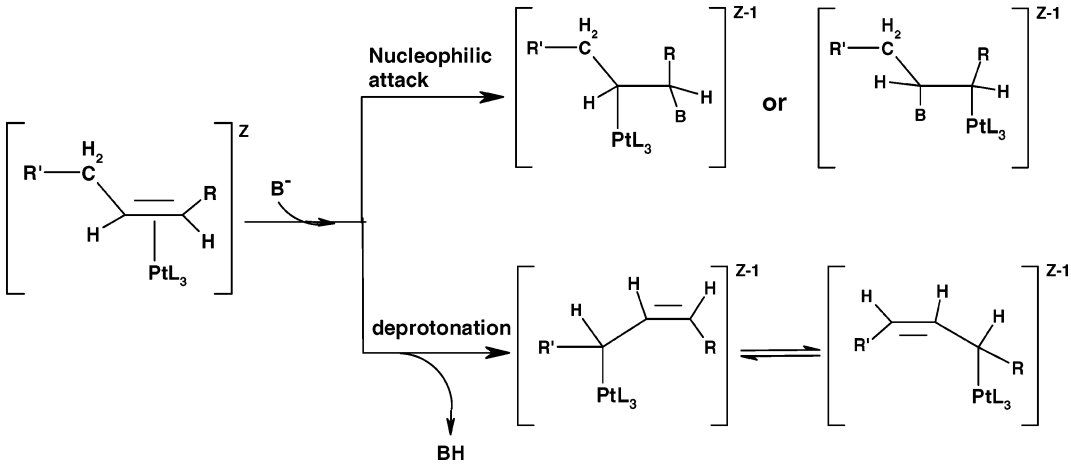

nucleophilicity of the bridging sulfur atoms together with the flexible hinge angle between the two $Pt^{II}S_2$ planes in $[L_2\{Pt(\mu\text{-}S)_2Pt\}L_2]$ (L = phosphine) metalloligands account for (a) their outstanding behavior as precursors to a large family of homo- and heterometallic complexes;[8] (b) their spontaneous evolution in the presence of organic electrophilic agents, such as CH_2Cl_2;[9] (c) the cascade of reactions following protonation of the bridging sulfur atoms in $\{Pt_2S_2\}$;[10] and (d) the first evidence of fast intramolecular S−H···S proton transfer in a transition metal complex.[11] Thus, on the basis of the high electron density on the sulfur atoms in $[L_2\{Pt(\mu\text{-}S)_2Pt\}L_2]$ compounds, it was reasonable to expect that their coordination to a $\{Pt^{II}(cod)\}$ fragment should have an effect on the electrophilicity of the cod ligand and possibly modify the reactivity of the $\{Pt^{II}(cod)\}$ fragment toward attack by nucleophiles.

In this paper we report the synthesis and characterization of $[\{Pt_2(\mu_3\text{-}S)_2(dppp)_2\}Pt(cod)]Cl_2$ (**1**) and $[\{Pt_2(\mu_3\text{-}S)_2(cod)_2\}Pt(dppp)]Cl_2$ (**3**), whose cationic species contain one or two $\{Pt^{II}(cod)\}$ fragments, respectively. Both cations, in contrast with the general behavior of cationic olefin complexes of platinum, do not undergo spontaneous loss of the unsaturated ligand and, thus, have allowed exploration of their reactivity toward a strong nucleophile such as $NaCH_3O$. Unlike previous reports on the attack of $NaCH_3O$ on the $\{Pt^{II}(cod)\}$ fragment,[12] the above reactions have not promoted the nucleophilic attack of the methoxide anion, but only deprotonation of cod, thus leading to $[\{Pt_2(\mu_3\text{-}S)_2(dppp)_2\}Pt(C_8H_{11})]Cl$ (**2**), $[\{Pt_2(\mu_3\text{-}S)_2(cod)(C_8H_{11})\}Pt(dppp)]Cl$ (**4**), and $[\{Pt_2(\mu_3\text{-}S)_2(C_8H_{11})_2\}Pt(dppp)]$ (**5**). In addition, the replacement of cod by dppp in complexes **1**−**4** has been studied. Overall, a combination of experimental data and theoretical calculations shows the noninnocent role of the $[(dppp)\{Pt(\mu\text{-}S)_2Pt\}(dppp)]$ metalloligand on the reactivity of the platinum-bonded olefin.

Results and Discussion

Experimental Results. The sequence of reactions carried out in this study is shown in Scheme 2. NMR parameters and mass determinations for the complexes **1**−**5** thus obtained are given in Table 1. Details of the synthetic pathways followed are given in the Experimental Section.

Complex **1** was formed as the only product of the following reaction in benzene solution:

$$[(dppp)\{Pt(\mu\text{-}S)_2Pt\}(dppp)] + [PtCl_2(cod)] \rightarrow [\{Pt_2(\mu_3\text{-}S)_2(dppp)_2\}Pt(cod)]Cl_2\ (\mathbf{1})\quad (A)$$

Remarkably, all attempts to replace the cod ligand in **1** by dppp or chloride anions were unsuccessful. Thus, different reaction conditions, such as the solvent and temperature of the reaction as well as the molar ratio of the reagents, never led to the already known $[Pt_3(\mu_3\text{-}S)_2(dppp)_3]Cl_2$ complex.[10] These observations are consistent with previously reported results for related compounds containing the $\{Rh^{I}(cod)\}$ fragment bonded to a $\{Pt_2(\mu\text{-}S)_2\}$ core, $[\{Pt_2(\mu_3\text{-}S)_2(PPh_3)_4\}Rh(cod)]^+$ and $[\{Pt_2(\mu_3\text{-}S)_2(\text{-}diop)_2\}Rh(cod)]^+$.[13] However, in contrast to the striking stability toward substitution of the cod ligand in **1**, this complex reacts with $NaCH_3O$ or Na_2S under mild conditions, affording $[\{Pt_2(\mu_3\text{-}S)_2(dppp)_2\}Pt(C_8H_{11})]Cl$ (**2**). While this formula agreed well with the ESI MS and MALDI TOF parameters of **2** in solution, the coordinative behavior of the deprotonated cod ligand, $(C_8H_{11})^-$, was deduced from the DEPT-135 NMR spectrum, displaying five different CH and three different CH_2 groups. $^{13}C-^{195}Pt$ couplings have been observed for the signals at $\delta = 83.29$ ($^1J_{Pt-C} = 144$ Hz) and 81.35 ($^1J_{Pt-C} = 176$ Hz), which can thus be assigned

(8) (a) Fong, S.-W. A.; Hor, T. S. A. *J. Chem. Soc., Dalton Trans.* **1999**, 639, and references therein. (b) Capdevila, M.; Carrasco, Y.; Clegg, W.; Coxall, R. A.; González-Duarte, P.; Lledós, A.; Ramírez, J. A. *J. Chem. Soc., Dalton Trans.* **1999**, 3103. (c) Yam, V. W.-W.; Yeung, P. K.-Y.; Cheung, K.-K. *Angew. Chem Int. Ed. Engl.* **1996**, *35*, 739.

(9) Mas-Ballesté, R.; Capdevila, M.; Champkin, P. A.; Clegg, W.; Coxall, R. A.; Lledós, A.; Mégret, C.; González-Duarte, P. *Inorg. Chem.* **2002**, *41*, 3218.

(10) Mas-Ballesté, R.; Aullón, G.; Champkin, P. A.; Clegg, W.; Mégret, C.; González-Duarte, P.; Lledós, A. *Chem. Eur. J.* **2003**, *9*, 5023.

(11) Aullón, G.; Capdevila, M.; Clegg, W.; González-Duarte, P.; Lledós, A.; Mas-Ballesté, R. *Angew. Chem., Int. Ed.* **2002**, *41*, 2776.

(12) (a) Aucott, S. M.; Slawin, A. M. Z.; Wollins, J. D. *J. Chem. Soc., Dalton Trans.* **2000**, 2559. (b) Bhattacharyya, P.; Slawin, A. M. Z.; Smith, M. B. *J. Chem. Soc., Dalton Trans.* **1998**, 2467. (c) Slawin, A. M. Z.; Smith M. B.; Wollins, J. D. *J. Chem. Soc., Dalton Trans.* **1996**, 3659. (d) Giordano, F.; Vitagliano, A. *Inorg. Chem.* **1981**, *20*, 633. (e) Bamberi, G.; Forsellini, E.; Gonziani, R. *J. Chem. Soc., Dalton Trans.* **1972**, 525.

(13) (a) Brunner, H.; Weber, M.; Zabel, M. *J. Organomet. Chem.* **2003**, *684*, 6. (b) Briant, C. E.; Gilmour, D. I.; Luke, M. A.; Mingos, D. M. P. *J. Chem. Soc., Dalton Trans.* **1985**, 851.

Scheme 2

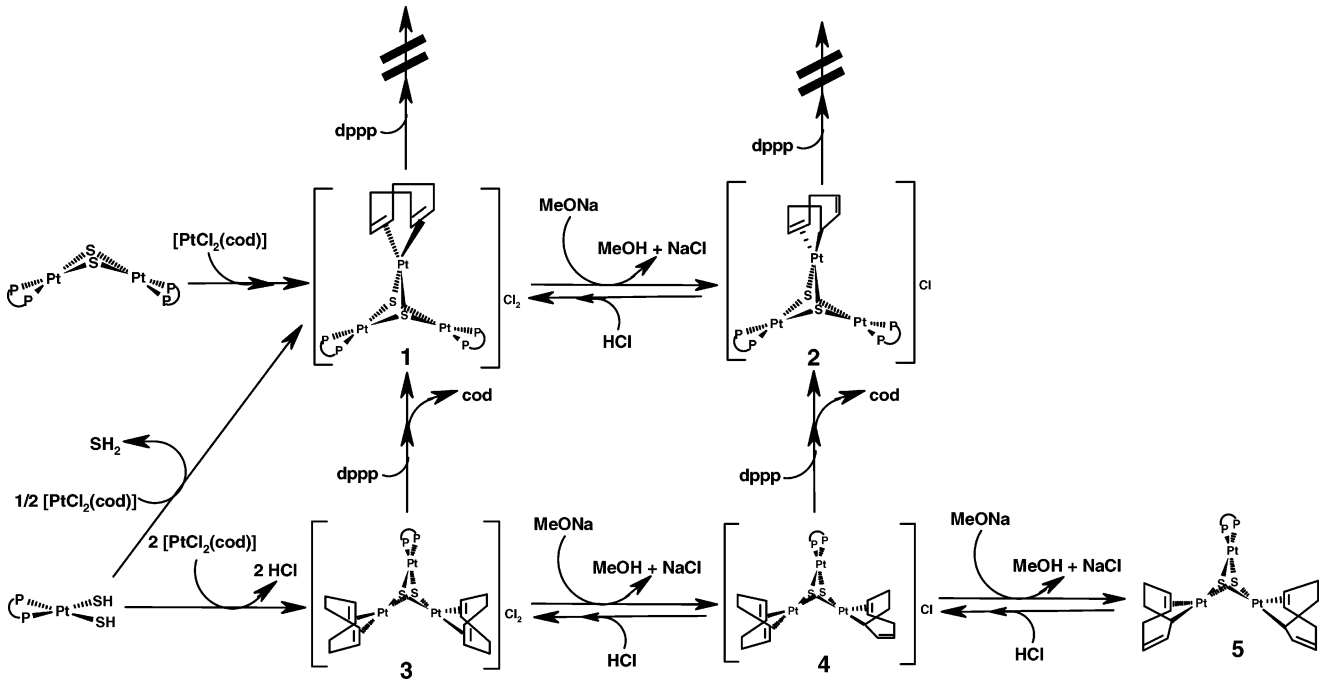

Table 1. NMR Parameters and Mass Determinations for Complexes 1−5

complex	mass data (ESI and/ or MALDI)	calculated MW	$\delta(^{31}P)$, ppm[a]	$^1J_{Pt-P}$, Hz	$\delta(^1H)$ of cod ligand, ppm[a]	$\delta(^{13}C)$ of cod ligand, ppm[a]
$[Pt_2(\mu\text{-}S)_2(dppp)_2]$	1279 (ESI)	1279.1	−0.1	2615		
1	790.9[b] (ESI)	1582.4	−4.1	3069	4.54 (CH), 2.53 (CH_2)	96.9 (CH), 29.8 (CH_2)
2	790.5[c] (ESI) 1581.1 (MALDI)	1581.4	−6.3	3006	4.27 (CH), 4.04 (CH), 3.09 (CH), 2.81 (CH), 2.27 (CH), 2.82 (CH_2), 2.01 (m, CH_2)	83.3 (CH, $^1J_{Pt-C}$ = 144 Hz), 81.3 (CH, $^1J_{Pt-C}$ = 176 Hz), 75.2 (CH, $^1J_{Pt-C}$ = 598 Hz), 54.2 (CH), 26.3 (CH), 33.9 (CH_2), 29.0 (CH_2), 28.3 (CH_2)
$[Pt(SH)_2(dppp)]$	640.1[d] (ESI)	673.6	−1.3	2760		
3	638.9[b] (ESI)	1278.1	−2.6	3193	5.49 (CH), 4.99 (CH), 2.5 (m, CH_2)	101.0 (CH), 98.8 (CH), 30.1 (CH_2)
4	638.7[c] (ESI) 1277.1 (MALDI)	1277.1	−3.7 (m)		5.3−5.1 (br, CH), 4.8−4.6 (br, CH)	96.4−95.0 (m, CH), 85.2 (CH), 84.5 (CH), 83.4 (CH), 83.2 (CH), 79.0 (CH), 78.3 (CH), 54.6 (CH), 54.5 (CH), 28.0 (CH), 27.3 (CH) 34.5 (CH_2), 34.2 (CH_2), 30.5−29.7 (m, CH_2), 28.9 (CH_2), 28.8 (CH_2), 28.5 (CH_2), 28.1 (CH_2)
5	638.9[c] (ESI) t1276.9 (MALDI)	1276.1	−6.1 (m)		5.2−3.8 (br, m, CH)	85.1−83.2 (m, CH), 79.2−78.0 (m, CH), 73.1−72.3 (m, CH), 54.4−54.1 (m, CH), 26.8−25.3 (m, CH); 35.6−34.3 (m, CH_2), 29.4−27.8 (m, CH_2)

[a] All ^{31}P, ^1H, and DEPT-135 ^{13}C NMR spectra were recorded in d_6-dmso solution. Abbreviations: m, multiplet; br, broad. [b] $M^{2+}/2$. [c] Protonated species as a result of the formic acid added in ESI-MS measurements. [d] $[(dppp)Pt(SH)]^+$ fragment.

to a platinum(II)-coordinated double bond, and for the signal at $\delta = 75.18$ ($^1J_{Pt-C} = 598$ Hz) corresponding to a σ-coordinated carbon atom. These features are consistent with $(C_8H_{11})^-$ being bound to platinum(II) by means of one η^2-alkene and one η^1-allyl bond. Full structural characterization of **2** has required a combination of crystallography and theoretical calculations, both discussed below. On the basis of the three sets of data (NMR, X-ray, and theoretical calculations) it has been deduced that the isomer labeled as allyl A in Figure 1 corresponds to **2** either in the solid phase or in solution.

Interestingly, the reaction leading from **1** to **2** can easily be reversed. Thus, addition of a stoichiometric amount of dilute HCl to a solution of **2** converts it to **1**.

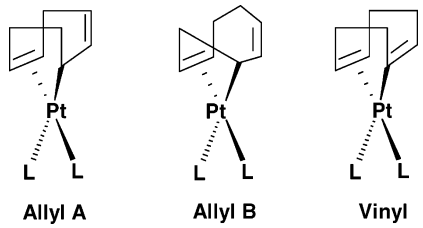

Figure 1. Possible binding modes of the $(C_8H_{11})^-$ ligand in a $[L_2Pt(C_8H_{11})]$ complex.

The ^2H NMR spectrum of a solution of **2** after addition of DCl instead of HCl reveals an allylic position for the added hydrogen atom and thus confirms that the base-

promoted deprotonation of cod in **1** corresponds to a C−H allylic activation. Additionally, we have observed that the behavior of the anionic deprotonated $(C_8H_{11})^-$ ligand in **2** toward replacement by dppp or chloride anions is comparable to that of neutral cod in **1**, both being substitutionally inert ligands.

Complex **3**, an analogue of **1**, but with one dppp ligand replaced by cod, has been obtained in accordance with the reaction:

$$[Pt(SH)_2(dppp)] + 2[PtCl_2(cod)] \rightarrow [\{Pt_2(\mu_3\text{-}S)_2(cod)_2\}Pt(dppp)]Cl_2\ (\mathbf{3}) + 2HCl \quad (B)$$

which requires the slow addition of a solution of $[Pt(SH)_2(dppp)]$ to a solution of $[PtCl_2(cod)]$, so that an excess of the latter reagent is always present in the reaction medium. Otherwise, a mixture of complexes **1** and **3** is obtained, formation of **1** probably being due to the reaction

$$2[Pt(SH)_2(dppp)] + [PtCl_2(cod)] \rightarrow [\{Pt_2(\mu_3\text{-}S)_2(dppp)_2\}Pt(cod)]Cl_2\ (\mathbf{1}) + 2SH_2 \quad (C)$$

Overall, reactions A and B lead to pure complexes **1** and **3**, respectively, under the experimental conditions here described. A mixture of both **1** and **3** has been obtained only if reactions B and C are allowed to proceed simultaneously, which requires the presence of $[Pt(SH)_2(dppp)]$ as well as a $[Pt(SH)_2(dppp)]/[PtCl_2(cod)]$ ratio greater than 1:2. Notably, the reaction of $[Pt_2(\mu\text{-}Se)_2(PPh_3)_4]$ with $[PtCl_2(cod)]$, which is comparable to reaction A, affords a mixture of $[\{Pt_2(\mu_3\text{-}Se)_2(PPh_3)_4\}Pt(cod)]^{2+}$ and $[\{Pt_2(\mu_3\text{-}Se)_2(cod)_2\}Pt(PPh_3)_2]^{2+}$, closely related to **1** and **3**, respectively.[14]

The acid−base reactions involving **3** compare well with those of **1**. Thus, the addition of 1 equiv of $NaCH_3O$ to a solution of **3** yields $[\{Pt_2(\mu_3\text{-}S)_2(cod)(C_8H_{11})\}Pt(dppp)]Cl$ (**4**), which, after subsequent additions of base, evolves to $[\{Pt_2(\mu_3\text{-}S)_2(C_8H_{11})_2\}Pt(dppp)]$ (**5**). Within the same context of the acid−base chemistry, the reactions from **3** to **4**, and eventually to **5**, are easily reversed by addition of the corresponding amount of dilute hydrochloric acid. With respect to the binding modes of the $(C_8H_{11})^-$ ligands in **4** and **5**, ^{13}C DEPT 135 NMR data clearly indicate that they all bind to platinum(II) by means of one η^2-alkene and one η^1-allyl bond, as already found in **2**. As theoretical calculations for the latter complex and other model compounds show that the allyl A isomeric form (Figure 1) has the greatest stability (described below), the same disposition has been assumed for all $(C_8H_{11})^-$ ligands in **4** and **5**.

The replacement reaction of cod by dppp ligands in **3** and **4** shows marked differences from the results observed for the same reaction with **1** and **2**. Thus, the reaction of **3** with dppp promotes replacement of one of the two cod ligands and leads to **1**. That of **4** with dppp entails substitution of the uncharged cod ligand only and yields **2**. These results indicate that **1** and **2** are particularly stable complexes, not only substitutionally inert, but also the only products obtained in the reaction of **3** and **4** with dppp. Comparison of both families of complexes (**1**, **2** vs **3**, **4**) clearly indicates that the presence of the $[(dppp)\{Pt(\mu\text{-}S)_2Pt\}(dppp)]$ moiety is responsible for the outstanding stability of **1** and **2**.

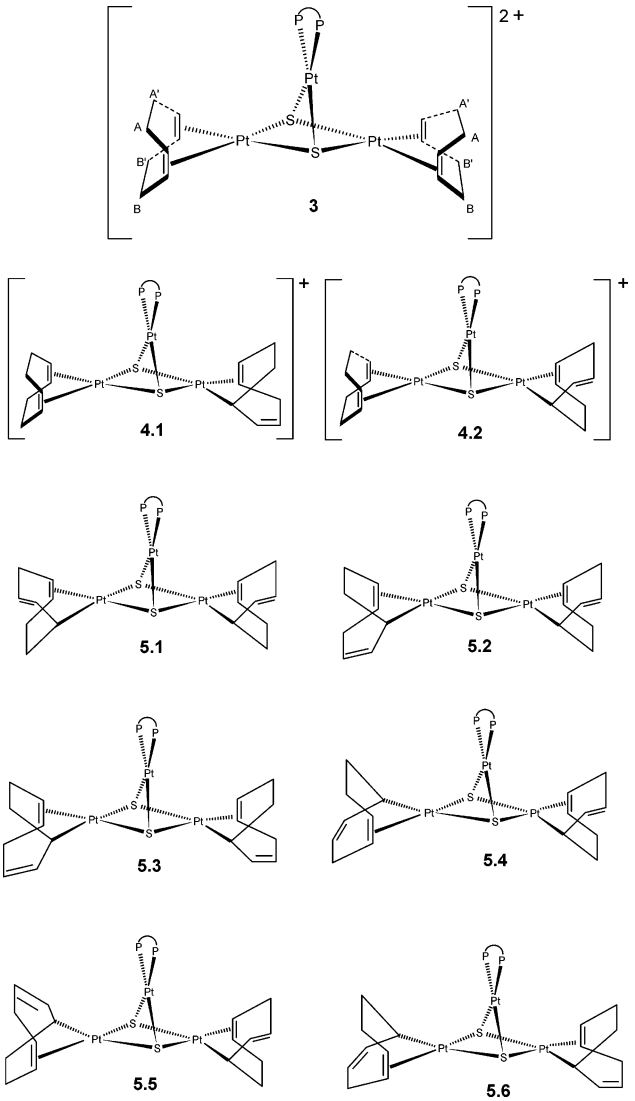

Figure 2. Labeling of the carbon atoms of cod ligand in **3** and possible isomers of **4** and **5**.

NMR characterization of complexes **4** and **5** requires consideration of their corresponding isomeric forms, which are depicted in Figure 2. In addition, the NMR parameters of the related complexes **1**−**3** provide a reference for a comparative analysis. All NMR data are given in Table 1. Thus, the $^{13}C\{^1H\}$ and ^1H NMR spectra provide evidence that the carbon and hydrogen atoms of cod in **3**, in contrast to **1**, are not symmetrically equivalent, as shown by the two groups of signals assigned to the CH groups. Consequently, deprotonation of cod in **3** to afford **4** gives rise to two isomers as long as the binding behavior of $(C_8H_{11})^-$ corresponds to the allyl A form exclusively. This assumption is fully validated by the ^{13}C DEPT 135 NMR spectrum of **4**, which displays two sets of signals corresponding to the deprotonated $(C_8H_{11})^-$ ligand, each set including five CH and three CH_2 groups. These data not only denote two different dispositions of the $(C_8H_{11})^-$ ligand in **4** but also show that their binding to platinum occurs by means of η^2-alkene and η^1-allyl coordination modes. The choice of the allyl A with respect to the allyl B form is discussed

(14) Yeo, J. S. L.; Vittal, J. J.; Henderson, W.; Hor, T. S. A. *Inorg. Chem.* **2002**, *41*, 1194.

Table 2. Relative Energies (kcal/mol) for the Different Isomers of Complexes $[L_2Pt(C_8H_{11})]$

	gas phase			solution[a]		
	allyl (A)	allyl (B)	vinyl	allyl (A)	allyl (B)	vinyl
2 Cl^-	0.0	5.4	31.7	0.0	3.1	28.9
2 SH^-	0.0	4.6	29.8	0.0	4.2	27.3
$[Pt_2(\mu\text{-}S)_2(PH_3)_4]$	0.0	7.8	34.7	0.0	7.1	32.9
2 PH_3	0.0	5.5	27.4	0.0	4.4	27.3
2 SH_2	0.0	7.3	32.3	0.0	6.4	32.5

[a] Calculated in methanol ($\epsilon = 32.63$) using the COSMO continuum solvation model.

below. The coexistence of isomers **4.1** and **4.2** (Figure 2) in solution is corroborated by the $^{31}P\{^1H\}$ NMR of **4** showing two superimposed double doublets.

Following the same lines of reasoning as above, deprotonation of the two cod ligands in **3** should give rise to **5** in six isomeric forms, as shown in Figure 2. The coexistence in solution of all or several of these isomers accounts for the multiplet signal displayed for each carbon nucleus of $(C_8H_{11})^-$ in the $^{13}C\{^1H\}$ NMR spectra. In parallel, the $^{31}P\{^1H\}$ NMR spectrum of **5** consists of a broad signal.

Theoretical Study

Binding Mode of the $(C_8H_{11})^-$ Ligand. Deprotonation of the cod ligand can occur via a vinylic or an allylic proton, thus giving rise to different coordination modes of the $(C_8H_{11})^-$ ligand. Whereas in the former case only one isomer can be obtained (*vinyl* in Figure 1), the abstraction of an allylic proton can generate two isomers, depending on which of the two terminal allyl carbon atoms is bonded to the metal (allyl A and allyl B in Figure 1). Thus, three different isomers must be considered. The relative stabilities of these isomers in the gas phase and in methanol solution were evaluated for a series of $[L_2Pt(COD)]^z$ ($z = 0$, $L_2 = 2SH^-$, $2Cl^-$; $z = +2$, $L_2 = [Pt_2(\mu\text{-}S)_2(PH_3)_2]$, $2PH_3$, and $2SH_2$) complexes (Table 2). The relative stabilities of the three isomers are practically the same for all the complexes studied, both in the gas phase and in solution. The total charge of the complex does not affect the relative stabilities: very similar relative energies among the isomers are obtained for the neutral and dicationic species. The vinyl isomer is highly unstable compared to both allylic isomers. Regarding the two allylic isomers, for all the complexes studied allyl A is more stable than allyl B by a range of 4.5−8 kcal/mol in the gas phase and 3−7 kcal/mol in solution. The coordination geometry of the platinum center in isomer B shows a high distortion from planarity. In contrast, isomer A presents a less strained structure. These structural features could explain the higher stability of isomer A.

The relative energies calculated for a model of complex **2** ($L_2 = [Pt_2(\mu\text{-}S)_2(PH_3)_2]$) fully agree with the complete series of the studied complexes. From these theoretical values, the vinyl isomer can be discarded, in agreement with the spectroscopic data indicating that the product of the deprotonation reaction contains a Pt-allyl group. Moroever, the allyl A isomer can be proposed as the observed isomer for complex **2**, and the preference for this binding mode of the $(C_8H_{11})^-$ ligand can be extended to complexes **4** and **5**.

Stability of $[L_2Pt(cod)]^z$ ($z = 0, +2$) Complexes toward cod Displacement. The cod ligand is usually a somewhat labile ligand, which can be displaced easily by ligands with higher coordinating ability such as bidentate phosphines. However, this is not the case in compound **1**. To elucidate the reasons for the surprising stability of the cod ligand in **1** toward substitution by dppp, the reaction energy (ΔE_{LE}) for the ligand exchange reaction (D) has been calculated for a series of eight related $[L_2Pt(cod)]^z$ complexes, taking $H_2P\text{-}(CH_2)_3\text{-}PH_2$ (dhpp) as a model of the dppp ligand.

$$[L_2Pt(cod)]^z + dppp \rightarrow [L_2Pt(dppp)]^z + cod \quad (D)$$

The complexes of the series are neutral ($z = 0$) when L ligands are SH^-, I^-, Br^-, or Cl^-, and cationic ($z = +2$) when L ligands are PH_3, SH_2, $[Pt_2(\mu\text{-}S)_2(dhpp)_2]$ (complex **1**), or $[Pt_2(\mu\text{-}S)_2(dhpp)(cod)]$ (complex **3**). Consideration of a series of $[L_2Pt(cod)]$ complexes with ligands L of different natures should enable us to put the energetic values for the ligand exchange obtained for complexes **1** and **3** into a general context. The computed ΔE_{LE} values are shown in Table 3.

The results indicate that substitution of cod by dppp is, in all studied cases, highly favored on thermodynamic grounds. The process is highly exothermic, with ΔE_{LE} ranging from −18.7 to −37.5 kcal/mol. The substitution of a cod ligand by dppp is more exothermic for cationic complexes than for neutral ones; this statement agrees well with the higher lability of olefinic ligands generally observed for cationic Pt-alkene complexes.[5] Our results justify the replacement of cod by dppp ligands observed in **3** and **4**, but they cannot explain the stability toward cod displacement exhibited by complex **1**. Indeed they suggest that the factors hampering the exchange of the cod ligand by dppp in **1** should be of a kinetic nature.

The bond dissociation energies (BDEs) for cod and dppp ligands in this series of complexes were also evaluated (see Table 3). Determination of these thermodynamic parameters can provide a mechanistic insight, because BDEs give an approximate estimation of the energy barrier for a dissociative ligand-exchange process. The results presented here show that the Pt−cod bond energies are higher for cationic $[L_2Pt(cod)]$ complexes than for neutral ones. High and similar values of BDE_{Pt-cod} have been calculated for cationic complexes with $L_2 = [Pt_2(\mu\text{-}S)_2(dhpp)_2]$ and $[Pt_2(\mu\text{-}S)_2(dhpp)(cod)]$, despite the very different behavior toward the cod/dppp exchange observed in **1** and **3**. The high BDE_{Pt-cod} obtained indicates that the dissociative mech-

Table 3. Reaction Energies for the cod/dppp Ligand Exchange Reaction and Pt-cod and Pt-dppp Bond Dissociation Energies in $[L_2Pt(cod)]$ Complexes (in kcal/mol)

L_2	$2SH^-$	$2I^-$	$2Br^-$	$2Cl^-$	$[Pt_2(\mu\text{-}S)_2(dhpp)_2]$[a]	$[Pt_2(\mu\text{-}S)_2(dhpp)(cod)]$	$2PH_3$	$2SH_2$
ΔE_{LE}	−18.7	−23.7	−23.2	−22.5	−28.2	−28.7	−33.6	−37.5
$BDE_{(Pt-cod)}$	42.2	57.4	65.5	73.6	78.9	81.7	116.5	140.1
$BDE_{(Pt-dppp)}$	60.7	81.1	88.7	96.1	107.1	110.4	150.1	177.6

[a] dhpp = $H_2P(CH_2)_3PH_2$.

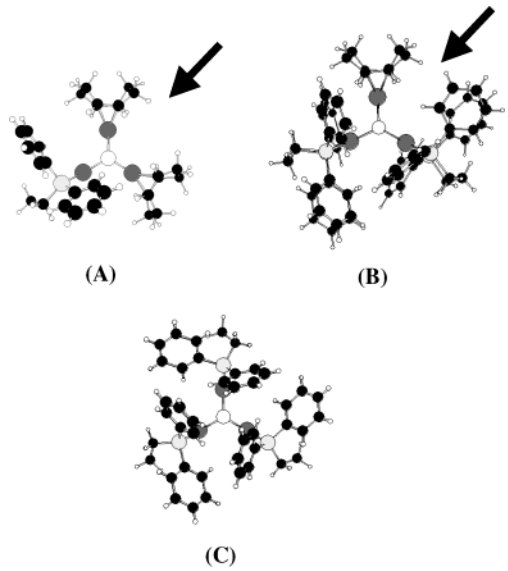

Figure 3. Molecular models of complexes $[\{Pt_2(\mu\text{-}S)_2(cod)_2\}Pt(dppp)]^{2+}$ (A), $[\{Pt_2(\mu\text{-}S)_2(dppp)_2\}Pt(cod)]^{2+}$ (B), and $[Pt_3(\mu_3\text{-}S)_2(dppp)_3]^{2+}$ (C). Arrows indicate the space available for the attack of an additional ligand.

anism is highly unfavorable in **1** and **3** and suggests an associative mechanism for the replacement of cod by dppp. This mechanistic proposal agrees with others found in the literature; for instance, the ligand exchange of olefins in d^8 square-planar complexes is supposed to go through an associative mechanism.[15] Nevertheless, associative mechanisms are subject to the achievability of a transition state with five ligands coexisting in the coordination sphere of the metal center. In the $[L_2Pt(cod)]^z$ complexes under study, when L is bulky, as for the $[Pt_2(\mu\text{-}S)_2(dppp)_2]$ metalloligand, the transition state for the associative mechanism would be highly unstable or may not even exist. Thus, the high steric hindrance due to $[Pt_2(\mu\text{-}S)_2(dppp)_2]$ in **1** hampers the associative mechanism for the replacement of cod ligand by dppp to yield $[Pt_3(\mu_3\text{-}S)_2(dppp)_3]$ and confers a remarkable kinetic stability toward cod dissociation on **1**. Molecular models of the reactant ($[\{Pt_2(\mu_3\text{-}S)_2(dppp)_2\}Pt(cod)]^{+2}$) and product ($[Pt_3(\mu_3\text{-}S)_2(dppp)_3]^{+2}$) for the cod/dppp exchange reaction illustrate the difficulties encountered by dppp when approaching the platinum atom bound to cod and $[Pt_2(\mu\text{-}S)_2(dppp)_2]$ metalloligand simultaneously (Figure 3).

The cod/dppp ligand exchange is experimentally observed in **3**, bearing the metalloligand $[Pt_2(\mu\text{-}S)_2(dppp)(cod)]$. It is likely that, when cod has substituted one dppp ligand, the lower bulkiness of the metalloligand allows the associative mechanism to take place. The different hindrance imposed by the presence of cod or dppp in the $[Pt_2(\mu\text{-}S)_2(dppp)(L)]$ fragment can be inferred from Figure 3. In conclusion, the theoretical study indicates that, despite the replacement of cod by dppp in **1** to yield $[\{Pt_2(\mu_3\text{-}S)_2(dppp)_2\}Pt(dppp)]^{2+}$ being an exothermic process, the reaction is kinetically unfavorable because neither associative nor dissociative mechanisms are possible with a reasonable energetic barrier. This insight could be extended to the behavior of the reported complexes containing the $\{Pt_2(\mu_3\text{-}S)_2Rh(cod)\}^{2+}$ core, where cod has shown an enhanced stability toward ligand-exchange reactions.[13]

Table 4. Reaction Energies (in kcal/mol) for MeO^- Nucleophilic Attack or Deprotonation Reactions in $[L_2Pt(cod)]$ Complexes[a]

L_2	$2SH^-$	$2Cl^-$	$[Pt_2(\mu\text{-}S)_2(PH_3)_4]$	$2PH_3$	$2SH_2$
nucleophilic attack	−28.4	−41.3	−50.8	−62.9	−69.2
deprotonation	−12.7	−23.9	−40.0	−52.5	−58.5

[a] Calculated in methanol ($\epsilon = 32.63$) using the COSMO continuum solvation model.

Deprotonation versus Nucleophilic Attack on the cod Ligand. As far as the reactivity of complexes **1** and **3** toward MeO^- is concerned, the reaction proceeds with the abstraction of an allylic proton instead of the common nucleophilic attack of the methoxide anion on the double bond. DFT calculations using a continuum solvation model were carried out to try to understand this unexpected reactivity. The inclusion of solvent effects is mandatory to obtain a reliable estimation of reaction energies, given the changes in the charges experienced by the species throughout the reaction. The reaction energy for both processes, deprotonation (reaction E) and nucleophilic attack (reaction F) in methanol ($\epsilon = 32.63$), for a set of complexes of formula $[L_2Pt(cod)]^z$ ($z = 0$, $L_2 = 2SH^{--}$, $2Cl^-$; $z = +2$, $L_2 = [Pt_2(\mu\text{-}S)_2(PH_3)_2]$, $2PH_3$, and $2SH_2$) were evaluated (Table 4).

$$[L_2Pt(cod)]^z + CH_3O^- \rightarrow [L_2Pt(C_8H_{11})]^{z-1} + CH_3OH \quad \text{(E)}$$

$$[L_2Pt(cod)]^z + CH_3O^- \rightarrow [L_2Pt(C_8H_{12}OCH_3)]^{z-1} \quad \text{(F)}$$

These results show that, for all the different complexes studied, both reactions are highly exothermic, the cationic presenting a higher exothermicity than the neutral species. Comparing the reaction energies for both processes, the nucleophilic attack of methoxide anion on a cod double bond is thermodynamically more favorable than deprotonation for all the studied species. Nevertheless, these differences in the reaction energy are lower for cationic species than for neutral ones. Given these tendencies, although the nucleophilic attack is always thermodynamically favored, the deprotonation of the cod ligand becomes more feasible for cationic complexes. These features suggest that the experimentally observed reactivity for **1** and **3** toward MeO^-, giving rise to deprotonation, is a kinetically controlled process.

To evaluate the aforementioned hypothesis, the reaction profiles for the nucleophilic attack by the methoxide anion and the deprotonation of the cod ligand were calculated for two different $[L_2Pt(cod)]$ complexes, one neutral ($L_2 = 2Cl^-$) and one of a cationic nature ($L_2 = [Pt_2(\mu\text{-}S)_2(PH_3)_4]$). To study methoxide attack, the $C_{sp2}-O_{methoxide}$ distance was selected as the reaction coordinate. The reaction profiles for the nucleophilic attack found for both complexes in the gas phase and in methanol do not present any barrier. This is not a surprising result, which had already been found by Norrby et al. in a thorough theoretical study of nucleo-

(15) (a) Canovese, L.; Visentin, F.; Uguagliati, P.; Crociani, B. *J. Chem. Soc., Dalton Trans.* **1996**, 1921. (b) Johnson, L. K.; Killian, C. M.; Brookhart, M. *J. Am. Chem. Soc.* **1995**, *117*, 6414. (c) van Asselt, R.; Elsevier, C. J.; Smeets, W. J. J.; Spek A. L. *Inorg. Chem.* **1994**, *33*, 1521.

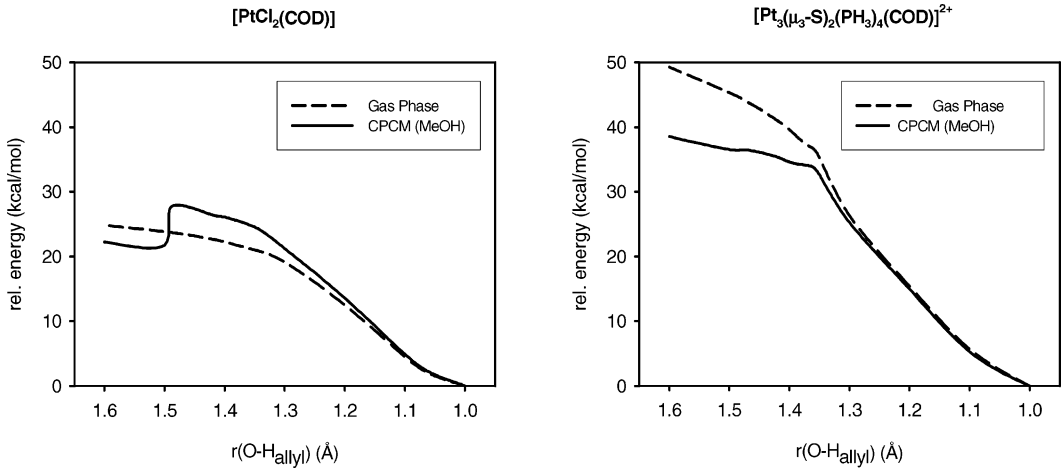

Figure 4. Deprotonation reaction profiles in gas phase and solution for complexes $[PtCl_2(cod)]$ and **1**.

philic attack on cationic (η^3-allyl)palladium complexes.[16] In this study, no transition state could be located for the reaction between an anionic nucleophile and a cationic (allyl)palladium complex. The authors concluded that this reaction does not have an energy barrier in the gas phase and that the barrier observed in real reactions can largely be attributed to the desolvation energy of the reacting ions. For the addition of anionic nucleophiles to cationic Pd-allyl complexes a transition state was found in solution only when constructing a two-dimensional potential energy surface.[16] The exploration of the bidimensional potential surface for the reactions under study greatly increases the computational requirements, and it is beyond the scope of this work.

The deprotonation reaction profiles in the gas phase and in solution for both complexes are shown in Figure 4. The selected reaction coordinate for this process is the $H_{allyl}-O_{methoxide}$ distance, which varies from 1.6 to 1.0 Å. In the case of the neutral $[Cl_2Pt(cod)]$ complex, the reaction has no barrier in the gas phase, whereas it shows an energy barrier of ca. 6 kcal/mol in solution. For the cationic $[Pt_2(\mu_3\text{-}S)_2(PH_3)_4\}Pt(cod)]^{2+}$ complex, the reaction does not present any barrier, either in the gas phase or in solution. To obtain more accurate reaction profiles, it would also be necessary to construct a two-dimensional potential energy surface in solution. Nevertheless, the exploration of these potential surfaces also demands too much computer time and was not performed.

Although the obtained results are not definitely conclusive, they can provide qualitative ideas about the unexpected reactivity exhibited by the cod ligand in **1**. The fact that in solution the cationic species do not present a barrier for proton abstraction, but neutral species do, suggests that deprotonation of **1** may be easier than that of $[Cl_2Pt(cod)]$. Moreover, although the nucleophilic attack is always thermodynamically more favorable than deprotonation, the energy differences between the two processes are reduced for cationic species, also suggesting that the deprotonation reaction is more feasible for cationic compounds. These results are consistent with the hypothesis that the observed reactivity of complex **1** with methoxide anion is a consequence of kinetic factors. It is likely that the bulkiness of the $[Pt_2(\mu\text{-}S)_2(dppp)_2]$ metalloligand causes steric interactions with the incoming nucleophile and also plays a role in favoring deprotonation.

(16) Hagelin, H.; Akermark, B.; Norrby, P.-O. *Chem. Eur. J.* **1999**, *5*, 902.

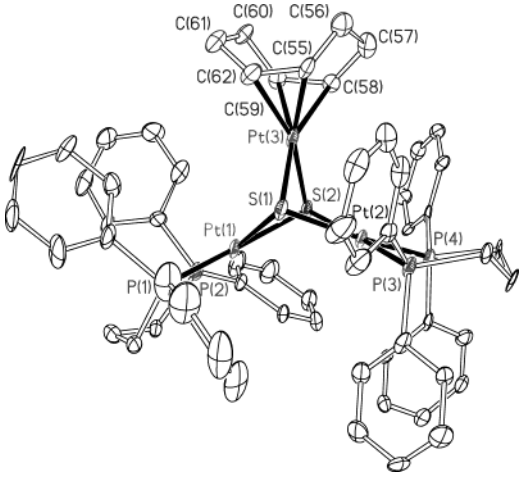

Figure 5. Molecular structure of **1** with the key atoms labeled and 50% probability ellipsoids. H atoms, Cl^-anions, and CH_3Cl solvent molecules have been omitted.

Table 5. Selected Bond Lengths (Å) and Angles (deg) for 1

Pt(1)−S(1)	2.375(4)	Pt(1)−S(2)	2.365(3)
Pt(2)−S(1)	2.372(3)	Pt(2)−S(2)	2.381(3)
Pt(3)−S(1)	2.342(3)	Pt(3)−S(2)	2.326(3)
Pt(1)−P(1)	2.261(3)	Pt(1)−P(2)	2.260(4)
Pt(2)−P(3)	2.263(3)	Pt(2)−P(4)	2.264(3)
Pt(3)−C(55)	2.195(13)	Pt(3)−C(58)	2.198(10)
Pt(3)−C(59)	2.218(10)	Pt(3)−C(62)	2.216(12)
C(55)−C(62)	1.346(16)	C(58)−C(59)	1.399(16)
S(1)−Pt(1)−S(2)	79.82(10)	S(1)−Pt(2)−S(2)	79.55(10)
S(1)−Pt(3)−S(2)	81.29(11)	P(1)−Pt(1)−P(2)	92.59(13)
P(3)−Pt(2)−P(4)	93.72(11)		

Molecular Structures

X-ray Crystal Structure of $[\{Pt_2(\mu_3\text{-}S)_2(dppp)_2\}Pt(cod)]Cl_2$ (1). The crystal structure of this complex consists of $[\{Pt_2(\mu_3\text{-}S)_2(dppp)_2\}Pt(cod)]^{2+}$ cations (Figure 5, Table 5) and Cl^- counterions held together by electrostatic interactions, and chloroform solvent molecules. The cation has no crystallographic symmetry, but has an approximately D_{3h} Pt_3S_2 core. The molecular

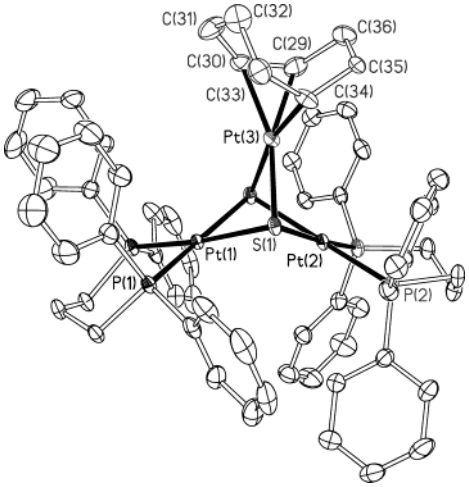

Figure 6. Molecular structure of **2** with the key atoms labeled and 50% probability ellipsoids. H atoms, ClO_4^- anions, and CH_2Cl_2 solvent molecules have been omitted.

structure of the trinuclear cation can be considered as formed by one [(dppp){Pt(μ-S)$_2$Pt}(dppp)] metalloligand linked to a {Pt(cod)} moiety through two sulfur atoms. The central Pt_3S_2 unit consists of a triangle of platinum atoms capped above and below by two sulfur atoms, thus describing a distorted trigonal bipyramid. These two triply bridging sulfido ligands lie essentially equidistant, 1.524 Å above and 1.516 Å below the Pt_3 plane. However, deviation from the ideal geometry is evidenced by the dihedral angles between pairs of the three PtS_2 planes, which range from 114.4° to 124.8°. The geometric features of the Pt_3S_2 unit compare well with those observed in the $[\{Pt_2(\mu_3\text{-}S)_2(dppp)_2\}Pt(C_8H_{11})]^+$ derivative, described below, and with related complexes containing the $P_6Pt_3S_2$ core with monodentate and chelating phosphine ligands.[8b,10,17] Moreover, the overall structure of $[\{Pt_2(\mu_3\text{-}S)_2(dppp)_2\}Pt(cod)]^{2+}$ bears a close resemblance to that of its selenium analogue containing a Pt_3Se_2 core.[14]

Each platinum atom in $[\{Pt_2(\mu_3\text{-}S)_2(dppp)_2\}Pt(cod)]^{2+}$ has square-planar coordination, distortion from the ideal geometry being mainly due to the reduction of the S−Pt−S angles from 90°. The two {PtS_2(dppp)} subunits show an antisymmetric arrangement of the PtP_2C_3 rings, both in a chair conformation, which become symmetry-equivalent in solution according to NMR data.

X-ray Crystal Structure of $[\{Pt_2(\mu_3\text{-}S)_2(dppp)_2\}Pt(C_8H_{11})](ClO_4)$ (2). The crystal structure of this complex consists of $[\{Pt_2(\mu_3\text{-}S)_2(dppp)_2\}Pt(C_8H_{11})]^+$ cations (Figure 6, Table 6) and ClO_4^- counterions held together by electrostatic interactions, and solvent molecules. The main structural features of the trinuclear cation can be described analogously to the parent $[\{Pt_2(\mu_3\text{-}S)_2(dppp)_2\}Pt(cod)]^{2+}$ complex, both consisting of a central Pt_3S_2 unit with a trigonal bipyramidal geometry. Distortion from the ideal geometry is slightly greater for $[\{Pt_2(\mu_3\text{-}S)_2(dppp)_2\}Pt(C_8H_{11})]^+$, where the dihedral angles between PtS_2 planes range from 112.7° to 125.7°.

Table 6. Selected Bond Lengths (Å) and Angles (deg) for 2

Pt(1)−S(1)	2.3592(11)	Pt(2)−S(1)	2.3705(11)
Pt(3)−S(1)	2.3789(11)	Pt(1)−P(1)	2.2558(11)
Pt(2)−P(2)	2.2519(12)	Pt(3)−C(29)	2.064(13)
Pt(3)−C(30)	2.103(10)	Pt(3)−C(34)	2.230(10)
S(1)−Pt(1)−S(1′)	81.42(5)	S(1)−Pt(2)−S(1′)	80.95(5)
S(1)−Pt(3)−S(1′)	80.60(5)	P(1)−Pt(1)−P(1′)	94.93(6)
P(2)−Pt(2)−P(2′)	95.72(6)		

However, the binding of the deprotonated cod ligand to platinum deserves special consideration, as disorder of this ligand and the solvent molecules across a mirror plane (which contains all three Pt atoms, bisects each diphosphine ligand, and relates the two bridging sulfide ligands to each other) resulted in serious overlap of the atomic arrangements (Figure 7) and hampered reliable determination of the C−C distances and positions of H atoms (see the Experimental Section for details of the disorder treatment). As shown in Figure 8, the C(29)−C(30) distance of 1.38 Å in the deprotonated cod ligand is consistent with a double bond and thus with one η^2-alkene binding mode of $(C_8H_{11})^-$ to platinum. Moreover, the Pt(3)−C(34) distance of 2.23 Å is compatible with a second coordination mode of either allylic (allyl A type) or vinylic nature. Concomitantly, the position of C(33), and thus the C(32)−C(33) and C(33)−C(34) distances, could be interpreted as indicative of an η^1-vinyl binding mode for the cod ligand, though the difference in these bond lengths is small (and insignificant statistically, in view of the relatively large standard uncertainties for these disordered atoms). In contrast, NMR data for $[\{Pt_2(\mu_3\text{-}S)_2(dppp)_2\}Pt(C_8H_{11})]^+$ are consistent with η^1-allyl rather than η^1-vinyl bonding, and DFT calculations show not only that the Pt(η^1-vinyl) coordination is strongly disfavored with respect to η^1-allyl but also that the allyl A isomer (Figure 1) is the energetically preferred form. Comparison of the structural data obtained by crystallography and DFT (Figure 8) shows that this apparent inconsistency is mainly due to the observed position of C(33), which is particularly affected by overlap with a solvent molecule in the disorder model and hence is especially unreliable. We thus deduce that the binding of $(C_8H_{11})^-$ to platinum probably occurs by means of η^2-alkene and η^1-allyl coordination modes in the solid state and in solution.

Concluding Remarks

The chemistry of $[\{Pt_2(\mu_3\text{-}S)_2(dppp)_2\}Pt(cod)]^{2+}$ has shown to be remarkable on the basis of (a) the high stability of the cod ligand toward substitutiton by dppp and (b) the ease of proton abstraction from the cod ligand as a result of the reaction with the methoxide anion. The preference of cod for deprotonation rather than the usual attack of the nucleophile on the olefinic bond is also shown in the reaction of $[\{Pt_2(\mu_3\text{-}S)_2(cod)_2\}Pt(dppp)]^{2+}$ and $[\{Pt_2(\mu_3\text{-}S)_2(cod)(C_8H_{11})\}Pt(dppp)]^+$ with sodium methoxide. Overall, the unprecedented behavior of cod in three cationic complexes containing a $[\{Pt_2(\mu_3\text{-}S)_2\}Pt(cod)]^{2+}$ moiety (as **1**, **3**, and **4**) reveals the strong influence of the $\{Pt_2(\mu\text{-}S)_2\}$ core on the reactivity of the $\{Pt(cod)\}^{2+}$ fragment. According to DFT calculations on a series of $[L_2Pt(cod)]^z$ species, the competition between proton abstraction and nucleophilic attack is highly dependent on the charge of the complex, the

(17) (a) Li, Z.; Mok, H. F.; Batsanov, A. S.; Howard, J. A. K.; Hor, T. S. A. *J. Organomet. Chem.* **1999**, *575*, 223. (b) Pilkington, M. J.; Slawin, A. M. Z.; Williams, D. J.; Woollins, J. D. *J. Chem. Soc., Dalton Trans.* **1992**, 2425. (c) Bushnell, G. W.; Dixon, K. R.; Ono, R.; Pidcock, A. *Can. J. Chem.* **1984**, *62*, 696.

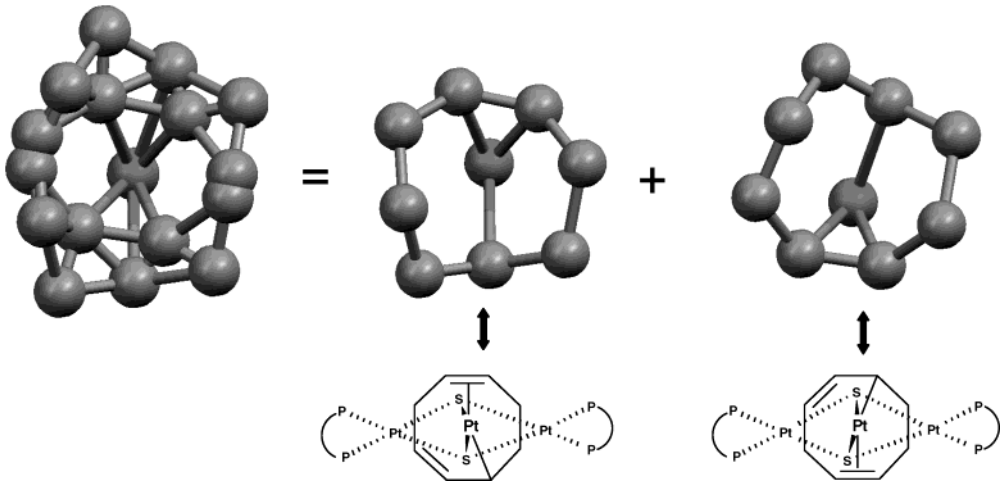

Figure 7. Representation of the overlap of atomic arrangements corresponding to the $\{Pt(C_8H_{11})\}$ fragment in **2**.

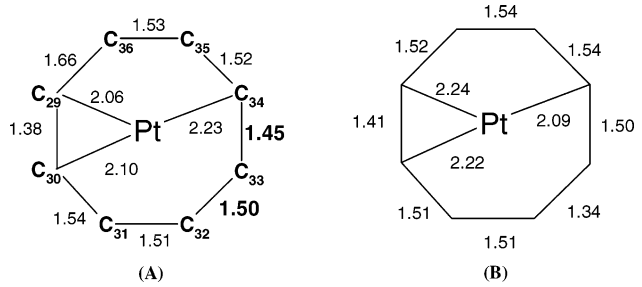

Figure 8. (A) Structural parameters obtained by X-ray diffraction for complex **2**. Numbers in bold characters are inconsistent with the proposal of an allyl A structure for the deprotonated cod ligand. (B) Structural parameters calculated by means of DFT calculations for the allyl A isomer.

former reaction appearing as more feasible in cationic (as **1** and **3**) than in neutral platinum complexes.

Concerning the substitution of cod (in neutral or anionic form) by dppp, the five complexes obtained behave differently. Those containing the $\{Pt_2(\mu_2\text{-}S)_2(dppp)_2\}$ moiety (as **1** and **2**) are substitutionally inert. By contrast, those based on the $\{Pt_2(\mu_2\text{-}S)_2(dppp)L\}$ moiety with L = cod or $C_8H_{11}^-$ (as **3**, **4**, and **5**) undergo the substitution reaction readily. However, DFT calculations show that replacement of cod by dppp in **1** or **3** is an exothermic process. Consequently, kinetic effects should account for the reluctance of cod to be replaced by dppp in **1** and **2**. These effects can be attributed to the steric hindrance imposed by the $\{Pt_2(\mu_2\text{-}S)_2(dppp)_2\}$ unit, which disfavors an associative pathway for the ligand exchange in **1**. This factor, combined with the high binding energy we have found for the cod ligand in a series of cationic platinum complexes, precludes the substitution of cod by dppp in **1**.

Finally, the unusual reactivity exhibited by the cod ligand in complexes containing the $[\{Pt(\mu_3\text{-}S)_2Pt\}Pt(cod)]^{2+}$ moiety and the dependence of such reactivity on electronic and steric factors involving the $\{Pt_2S_2\}$ core allow envisaging new perspectives. On the basis of the results here reported it can be proposed that the coordination of $[Pt_2(\mu\text{-}S)_2L_4]$ metalloligands to a transition metal ML_n' fragment can be an effective tool for modifying its chemical properties. In addition, these modifications could be modulated by a fine-tuning of the nature of the terminal ligands bound to the central $\{Pt_2S_2\}$ core.

Experimental Section

Materials and Methods. All reactions were carried out under an atmosphere of pure dinitrogen, and conventionally dried and degassed solvents were used throughout. These were Purex Analytical Grade from SDS. Solutions of NaOMe in MeOH (4.74 M) and DCl in D_2O (35 wt %, 99.9% D) were purchased from Aldrich. Metal complexes of formula $[PtCl_2(dppp)]$ and $[PtCl_2(cod)]$ were prepared according to published methods.[18] The synthesis of $[Pt(SH)_2(dppp)]$[10] and $[(dppp)Pt(\mu\text{-}S)_2Pt(dppp)]$[8b,9] has already been reported.

Complexes **1**−**5** have been characterized by NMR and mass spectroscopy. ^1H, $^{13}C\{^1H\}$, and $^{31}P\{^1H\}$ NMR spectra were recorded from samples in $(CD_3)_2SO$ solution at room temperature, using a Bruker AC250 spectrometer. ^{13}C and ^1H chemical shifts are relative to $SiMe_4$, and ^{31}P chemical shifts to external 85% H_3PO_4. The ^2H NMR spectra of the product reaction of **2** with DCl were recorded from $(CH_3)_2SO$ solution using a Bruker Avance500 spectrometer. The ESI MS measurements were performed on a VG Quattro Micromass instrument. Experimental conditions are given elsewhere.[9] MALDI mass spectra were obtained on a Voyager DE-RP (PerSeptive Biosystems, Framighan) time-of-flight (TOF) mass spectrometer equipped with a nitrogen laser (337 nm 3 ns pulse). The accelerating voltage in the ion source was 20 kV. Data were acquired in the reflector mode operation with a delay time value of 60 ns. Experiments were performed using the matrix 2,5-dihydroxybenzoic acid [DHB, Aldrich]. Matrix solutions were prepared by dissolving 10 mg of DHB in 10 mL of CH_3CN/H_2O 50% (v/v). Equal volumes (1 μL + 1 μL) of matrix solution and diluted samples (10^{-2} M in CH_3CN) were mixed and spotted onto the stainless steel sample plate. The mixture was dried in air before being introduced into the mass spectrometer. Elemental analyses were performed on a Carlo-Erba CHNS EA-1108 analyzer. However, as already found in some related phosphine platinum complexes,[9−11,19] microanalytical data referring to the carbon content in complexes **1**, **3**, and **4** were unsatisfactory.

Synthesis of $[\{Pt_2(\mu_3\text{-}S)_2(dppp)_2\}Pt(cod)]Cl_2$ (1). To a stirring solution of $[Pt_2(\mu_3\text{-}S)_2(dppp)_2]$ (0.5 g, 0.39 mmol) in benzene (100 mL) was added solid $[PtCl_2(cod)]$ (0.15 g, 0.39 mmol). The resulting clear solution was allowed to stir for 5 h at room temperature, during which time complex **1** formed as

(18) Brown, M. P.; Puddephatt, R. J.; Rashidi, M.; Seddon, K. R. *J. Chem. Soc., Dalton Trans.* **1977**, 951.
(19) Capdevila, M.; González-Duarte, P.; Foces-Foces, C.; Hernández Cano, F.; Martínez-Ripoll, M. *J. Chem. Soc., Dalton Trans.* **1990**, 143.

a white solid. Then, it was filtered off and washed with diethyl ether. Yield: 78%. X-ray quality crystals were grown by slow evaporation of a solution of **1** in $CHCl_3$. Anal. Calcd for $C_{62}H_{64}P_4Pt_3S_2Cl_2$: C, 45.04; H, 3.90; S, 3.88. Found: C, 44.21; H, 3.70; S, 3.74.

Synthesis of [{Pt$_2$(μ_3-S)$_2$(dppp)$_2$}Pt(C$_8$H$_{11}$)]Cl (2). To a suspension of **1** (0.5 g, 0.30 mmol) in benzene (75 mL) was added an equimolar amount of NaMeO in methanol (63 μL of a 4.74 M solution). After 8 h of stirring at room temperature the suspension was concentrated to ca. 20 mL under reduced pressure. Addition of diethyl ether to the filtrated solution yielded a pale yellow solid. Yield: 62%. X-ray quality crystals were obtained in CH_2Cl_2 after exchanging chloride by perchlorate anions. Anal. Calcd for $C_{62}H_{63}P_4Pt_3S_2Cl$: C, 46.06; H, 3.93; S, 3.97. Found: C, 45.62; H, 4.21; S, 3.63.

Synthesis of [{Pt$_2$(μ_3-S)$_2$(cod)$_2$}Pt(dppp)]Cl$_2$ (3). A solution of [Pt(SH)$_2$(dppp)] (0.22 g, 0.33 mmol) in benzene (50 mL) was added dropwise to a stirring solution of [PtCl$_2$(cod)] (0.25 g, 0.67 mmol) in the same solvent (50 mL) and the reaction mixture left to stir for 6 h at room temperature. After this time the solution was concentrated to ca. 25 mL and the yellow solid thus formed was filtered off and dried. Yield: 45%. Anal. Calcd for $C_{43}H_{50}P_2Pt_3S_2Cl_2$: C, 38.28; H, 3.74; S, 4.75. Found: C, 36.94; H, 3.89; S, 4.56.

Synthesis of [{Pt$_2$(μ_3-S)$_2$(cod)(C$_8$H$_{11}$)}Pt(dppp)]Cl (4). To a solution of **3** (0.10 g, 0.07 mmol) in benzene (25 mL) was added a methanol solution of NaMeO (17 μL of a 4.74 M solution). The resulting solution was left to stir for 4 h, after which time it was concentrated to ca. 5 mL and filtered. Addition of diethyl ether to the filtrate caused precipitation of complex **4** as a pale yellow solid. Yield: 28%. Anal. Calcd for $C_{43}H_{49}P_2Pt_3S_2Cl$: C, 39.35; H, 3.76; S, 4.88. Found: C, 37.67; H, 4.38; S, 5.19.

Synthesis of [{Pt$_2$(μ_3-S)$_2$(C$_8$H$_{11}$)$_2$}Pt(dppp)] (5). The same procedure as that followed for complex **4** yielded complex **5** from **3** (0.10 g, 0.074 mmol) and a methanol solution of NaMeO (43 μL of a 4.74 M solution). Yield: 31%. Anal. Calcd for $C_{43}H_{48}P_2Pt_3S_2$: C, 40.47; H, 3.79; S, 5.02. Found: C, 40.00; H, 4.15; S, 4.63.

Evolution with Time of a Solution of [{Pt$_2$(μ_3-S)$_2$(dppp)$_2$}Pt(cod)]Cl$_2$ (1) or [{Pt$_2$(μ_3-S)$_2$(dppp)$_2$}Pt(C$_8$H$_{11}$)]Cl (2) in the Presence of dppp. To a solution of complex **1** or **2** in either CH_2Cl_2, CH_3CN, or MeOH was added a 5:1 molar excess of dppp at room temperature. This solution was monitored for 48 h by taking one aliquot every 12 h, evaporating it to dryness, and recording the $^{31}P\{^1H\}$ NMR spectrum in d_6-dmso. The above experiments were also performed in the same solvents but under reflux conditions. NMR data revealed that the possible ligand exchange reactions did never occur.

Reaction between [{Pt$_2$(μ_3-S)$_2$(cod)$_2$}Pt(dppp)]Cl$_2$ (3) and dppp. To a solution of **3** (25 mg, 0.02 mmol) in CH_2Cl_2 (15 mL) was added dppp (8 mg, 0.02 mmol). After 2 h of stirring at room temperature the solvent was removed in vacuo, leaving the product as a white solid. The $^{31}P\{^1H\}$ NMR spectrum of this solid in d_6-dmso solvent showed that complex **1** was the only compound present in solution.

Reaction between [{Pt$_2$(μ_3-S)$_2$(cod)(C$_8$H$_{11}$)}Pt(dppp)]Cl (4) with dppp. To a solution of 0.02 g of **4** (0.015 mmol) in CH_2Cl_2 (15 mL) was added 8 mg (0.02 mmol) of dppp. After 2 h of stirring at room temperature the resulting solution was analyzed by $^{31}P\{^1H\}$ NMR as indicated above. The NMR data showed that complex **2** was the only compound present in solution.

Reaction between [{Pt$_2$(μ_3-S)$_2$(dppp)$_2$}Pt(C$_8$H$_{11}$)]Cl (2) and HCl or DCl. To a solution of **2** (0.20 g, 0.12 mmol) in benzene (25 mL) was added an equimolar amount of HCl in water (30 μL of a 4 M HCl solution). After 15 min of stirring at room temperature the solid formed was filtered off and analyzed by $^{31}P\{^1H\}$ NMR. These data confirmed that the only product obtained was complex **1**. Yield: 73%. The same experiment was carried out but with addition of an equimolar amount of DCl in D_2O (13 μL of a 9.3 M DCl solution) instead of HCl. The solid thus obtained was analyzed by $^{31}P\{^1H\}$ NMR, confirming complex **1** as the only product in both cases. In addition, the ^2H NMR spectrum of the compound obtained after addition of DCl shows a resonance at 2.47 ppm.

Reaction of [{Pt$_2$(μ_3-S)$_2$(cod)(C$_8$H$_{11}$)}Pt(dppp)]Cl (4) or [{Pt$_2$(μ_3-S)$_2$(C$_8$H$_{11}$)$_2$}Pt(dppp)] (5) with HCl. A solution containing 20 mg of **4** (0.015 mmol) or **5** (0.016 mmol) in CH_3CN (15 mL) was acidified by addition of 20 or 40 μL, respectively, of 1.0 M HCl in water. After 15 min of stirring at room temperature the solvent was evaporated to dryness. Characterization of the solid residue by $^{31}P\{^1H\}$ NMR indicated that complex **3** was the only end product in both acid−base reactions.

Table 7. Crystallographic Data for 1 and 2

	1	**2**
formula	$C_{62}H_{64}P_4Pt_3S_2^{2+}\cdot 2Cl^-\cdot 3CHCl_3$	$C_{62}H_{63}P_4Pt_3S_2^+\cdot ClO_4^-\cdot CH_2Cl_2$
fw	2011.4	1765.8
cryst syst	monoclinic	monoclinic
space group	$P2_1/n$	$P2_1/m$
a (Å)	13.5107(7)	12.8372(12)
b (Å)	20.5840(10)	14.8717(14)
c (Å)	28.7743(14)	19.6316(19)
β (deg)	99.474(2)	106.160(2)
V (Å^3)	7893.1(7)	3599.8(6)
Z	4	2
T (K)	160	120
no. of reflns measd	42 657	24 256
no. of unique reflns	10 305	10 158
R_{int}	0.078	0.041
R (F, $F^2 > 2\sigma$)	0.046	0.035
R_w (F^2, all data)	0.119	0.099
S (F^2, all data)	0.966	1.013
max., min. el dens (e Å^{-3})	1.61, −1.57	1.58, −1.71

X-ray Crystallography. Data for complexes **1** and **2** were measured on Bruker SMART 1K CCD diffractometers.[20] For **1**, Mo Kα radiation (λ = 0.71073 Å) was used, while the small size and poorly diffracting nature of the crystals of **2** necessitated the use of synchrotron radiation (λ = 0.6900 Å) at CCLRC Daresbury Laboratory SRS station 9.8.[21] Crystallographic data are given in Table 7. Both structures were found to contain solvent, some of which could be modeled with ordered atomic sites and some of which is disordered; for **1**, three ordered chloroform molecules were located, and other highly disordered solvent was handled by the SQUEEZE procedure in the program PLATON,[22] while for **2**, one ordered dichloromethane molecule was located (on a mirror plane), and other disordered solvent was fitted with a number of partially occupied atom sites giving no recognizable molecular geometry. For each structure, only the ordered solvent is included in the formulas given in Table 7. The cation of **2** lies on a crystallographic mirror plane, across which the deprotonated COD ligand lies. The atoms of the two disorder components and those of some of the disordered solvents overlap each other, rendering the geometry of these moieties unreliable. Restraints were applied to the anisotropic displacement parameters of the ligand, but no geometrical constraints or restraints were used for these atoms. The perchlorate anion is also disordered across a mirror plane. H atoms were included in ideal positions for ordered parts of both structures. Refinement was on all unique F^2 values in each case.[23] The largest features in final

(20) *SMART* and *SAINT* software; Bruker AXS Inc.: Madison, WI, 2001.

(21) Cernik, R. J.; Clegg, W.; Catlow, C. R. A.; Bushnell-Wye, G.; Flaherty, J. V.; Greaves, G. N.; Burrows, I.; Taylor, D. J.; Teat, S. J.; Hamichi, M. *J. Synchrotron Rad.* **1997**, *4*, 279.

(22) Spek, A. L. *PLATON*; University of Utrecht: The Netherlands, 2001.

(23) Sheldrick, G. M. *SHELXTL*, version 6; Bruker AXS Inc.: Madison, WI, 2001.

difference syntheses lie close to heavy atoms and disordered parts of the structures.

Computational Details. Calculations were performed using the GAUSSIAN98 series of programs.[24] Geometry optimizations were done using the density functional theory (DFT) with the hybrid B3LYP functional.[25] Effective core potentials (ECP) and their associated double-ζ LANL2DZ basis set were used for platinum, phosphorus, sulfur, iodine, bromine, and chlorine atoms,[26] adding an extra series of d-polarization functions in the case of P, S, I, Br, and Cl.[27] The 6-31G basis set was used for the C and H atoms.[28] Solvent effects were taken into account by means of the COSMO solvation model.[29] Energies were calculated with methanol ($\epsilon = 32.63$) as solvent, keeping the optimized geometry for the isolated species (single-point calculations).

Acknowledgment. Financial support from the Ministerio de Ciencia y Tecnología of Spain (projects BQU2001-1976 and BQU2002-04110-CO2-02), the EPSRC (UK), and Ineos Acrylics is gratefully acknowledged. R.M.B. is indebted to the Universitat Autònoma de Barcelona for a predoctoral scholarship.

Supporting Information Available: For **1** and **2**, details of crystal structure determination, atomic coordinates, bond lengths and angles, and displacement parameters. This material is available free of charge via the Internet at http://pubs.acs.org. Observed and calculated structure factor lists are available from the authors upon request.

OM034312X

(24) Frisch, M. J.; Trucks, G. W.; Schlegel, H. B.; Scuseria, G. E.; Robb, M. A.; Cheeseman, J. R.; Zakrzewski, V. G.; Montgomery, J. A., Jr.; Stratmann, R. E.; Burant, J. C.; Dapprich, S.; Millam, J. M.; Daniels, A. D.; Kudin, K. N.; Strain, M. C.; Farkas, O.; Tomasi, J.; Barone, V.; Cossi, M.; Cammi, R.; Mennucci, B.; Pomelli, C.; Adamo, C.; Clifford, S.; Ochterski, J.; Petersson, G. A.; Ayala, P. Y.; Cui, Q.; Morokuma, K.; Malick, D. K.; Rabuck, A. D.; Raghavachari, K.; Foresman, J. B.; Cioslowski, J.; Ortiz, J. V.; Stefanov, B. B.; Liu, G.; Liashenko, A.; Piskorz, P.; Komaromi, I.; Gomperts, R.; Martin, R. L.; Fox, D. J.; Keith, T.; Al-Laham, M. A.; Peng, C. Y.; Nanayakkara, A.; Gonzalez, C.; Challacombe, M.; Gill, P. M. W.; Johnson, B. G.; Chen, W.; Wong, M. W.; Andres, J. L.; Head-Gordon, M.; Replogle, E. S.; Pople, J. A. *Gaussian 98* (Revision A.7); Gaussian, Inc.: Pittsburgh, PA, 1998.

(25) (a) Becke, A. D. *J. Chem. Phys.* **1993**, *98*, 5648. (b) Lee, C.; Yang, W.; Parr, R. G. *Phys. Rev. B* **1988**, *37*, 785.

(26) (a) Hay, P. J.; Wadt, W. R. *J. Chem. Phys.* **1985**, *82*, 299. (b) Hay, P. J.; Wadt, W. R. *J. Chem. Phys.* **1985**, *82*, 270.

(27) Höllwarth, A.; Böhme, M.; Dapprich, S.; Ehlers, A. W.; Gobbi, A.; Jonas, V.; Köhler, K. F.; Stegman, R.; Veldkamp, A.; Frenking, G. *Chem. Phys. Lett.* **1993**, *208*, 237.

(28) Hehre, W. J.; Ditchfield, R.; Pople, J. A. *J. Chem. Phys.* **1972**, *56*, 2257.

(29) Barone, V.; Cossi, M. *J. Phys. Chem*, **1998**, *102*, 1995.